Calibration of a distributed hydrological model for simulations of remote glacierized Himalayan catchments using MODIS snow cover data

M. KONZ[1], D. FINGER[1], C. BÜRGI[1], S. NORMAND[1], W. W. IMMERZEEL[2,3], J. MERZ[4], A. GIRIRAJ[5] & P. BURLANDO[1]

1 *ETH Zurich, Institute of Environmental Engineering, Hydrology and Water Resources Management, Wolfgang-Pauli-Str. 15, 8093 Zurich, Switzerland*
markus.konz@ifu.baug.ethz.ch

2 *FutureWater, Wageningen, The Netherlands*

3 *Department of Physical Geography, Utrecht University, The Netherlands*

4 *INTEGRATION environment & energy, Kathmandu, Nepal*

5 *International Center for Integrated Mountain Development, ICIMOD, Kathmandu, Nepal*

Abstract The objective of this study is to investigate the suitability of remote sensing data to calibrate a distributed hydrological model of a Nepalese Himalayan headwater catchment. Snow cover data from the Moderate Resolution Imaging Spectroradiometer (MODIS) satellite are used to calibrate the snow and glacier routine of the conceptual hydrological model TAC^D. The snow cover information is useful to constrain the hydrological model in the calibration phase, especially in data-scarce regions. Simulation results using the MODIS calibrated parameter sets are evaluated against independent observations measured discharge data and glacier mass balance measurements of the Langtang Khola catchment. The constraint posed in the calibration phase by the spatially distributed observations allows a reduction in the equifinality problem, thus producing a better balance among the modelled processes and a more plausible partitioning of the different runoff components. Accordingly, we demonstrate that the use of a remote sensing-based additional source of information allows enhancing streamflow predictions for data scarce areas, thus also allowing water resources assessment in remotely located regions.

Key words multi-criteria calibration; MODIS snow cover data; Himalayan headwaters; modelling glacierized catchments

INTRODUCTION

The hydrology of mountain regions is highly important in many respects. Solid precipitation is permanently or seasonally stored as snow, and on longer time scales in glaciers, and contributes to the river streamflow with a seasonal delay. Such streamflow is available not only in mountainous regions, but it also contributes to the water supply of downstream lowlands, being in many cases the main available resource. According to Viviroli *et al.* (2007), the most important "water towers" of the world are located in arid and semi-arid regions where mountains contribute from 50 to 90% of total discharge, with extreme cases of >95%. This is, for instance, the case for the Himalayan headwaters, which supply a large part of the Indian flood plains, and for which an assessment in view of the effects of climate change is particularly important. However, such an assessment is often complicated by the limited availability of data due to the harsh conditions in high altitudes, and to difficulties in accessing the catchments.

Hydrological models can be used in place of observations to bridge the gap between available data and demand for prediction of hydrological processes, such as snow accumulation and ablation, runoff generation from rain and snow- and ice melt, which is necessary for water resources management. However, problems often arise in the simulation of glaciated catchments due to the high complexity of these environments. For instance, ice melt could be overestimated by the model, but a significant underestimation of precipitation input could compensate the errors of the melt simulations, or *vice versa*. It is thus important to develop techniques that allow model ambiguities to be minimized. In this respect Konz & Seibert (2010) have recently shown that, in addition to discharge observations, glacier mass balance data contain useful information to constrain the parameter sets (ps) of a model. However, glacier mass balance data are rarely available in the Himalayas. A substitute for them can be found in remotely sensed cryosphere data.

The Moderate Resolution Imaging Spectroradiometer (MODIS) snowcover products are increasingly used to study snow cover developments. Parajka & Blöschl (2006) validated MODIS snowcover data over the territory of Austria against *in situ* snow depth measurements, finding an accuracy of 95% with respect to ground observations on cloud-free days. Simic *et al.* (2004) compared MODIS and NOAA snow cover products with daily surface snow depth observations at about 2000 meteorological stations across Canada and found that both products have similar levels of agreement with ground data, with accuracies ranging from 80% to almost 100% on a monthly basis. In a more recent study Parajka & Blöschl (2008) demonstrated that the use of MODIS snow cover data improves the snow model performance when validated against independent ground snow depth data. Immerzeel *et al.* (2009) used MODIS products to identify spatial–temporal trends in snow cover across the entire Himalayas, and to model snowmelt runoff in the upper Indus basin. From all these studies it appears evident how remote sensing allows detection of spatial–temporal patterns of snow cover across large areas in inaccessible terrain, providing useful information on a critical component of the hydrological cycle in mountainous regions.

This paper aims at further developing the use of snowcover remote imagery by studying the applicability of MODIS snowcover data to constrain model parameter sets for hydrological simulations of discharge and other important water balance variables of remote Himalayan headwaters.

STUDY AREA

The Langtang River catchment (360 km^2, Table 1) is located approx. 100 km north of Kathmandu. The elevation ranges from 3800 m a.m.s.l. up to the peak of Langtang Lirung at 7234 m.a.s.l, with an average altitude of 5169 m a.m.s.l. Himalayan glaciers are summer accumulation-type glaciers, which means that both accumulation and ablation occur primarily during the summer monsoon season. The glaciers are categorized into two types, according to the surface conditions of the ablation zone: debris-free glaciers and debris-covered glaciers (Moribayashi, 1974). Of the 360-km^2 catchment area, 166 km^2 (46%) is occupied by glaciers, of which 32 km^2 (19%) are covered by debris, especially in the area of the glacier tongues below 5200 m.

Table 1 Features of the Langtang Khola catchment.

Area		
Total	(km^2)	360.0
Glacierized	(km^2/%)	164.4/45.7
Debris-covered glacier	(km^2/%)	32.1/19.5*[1]
Altitudes		
Range	(m a.m.s.l.)	3600–7234
Average	(m a.m.s.l.)	5158
Aspect		
North	(%)	21.4*[2]
South	(%)	26.8*[3]
East, West, Horizontal	(%)	51.9*[4]

*[1] in percent of glacier-covered area; *[2] 315–345°, *[3] 135–225°; *[4] 45–135° and 225–315°.

The main feature of the Nepalian climate is the monsoon circulation with predominant easterly winds in the summer and westerly winds from October to May. The pre-monsoon season, from March to mid-June, is characterized by a gradual increase of air temperature. The monsoon season, from mid-June to the end of September, is dominated by positive values of air temperature. In this season, diurnal variation of the air temperature is generally very small due to a thick cloud cover (Shiraiwa *et al.* 1992). The monsoon season is over at the end of September and is followed by the post-monsoon season, from October to December, which is characterized by fine weather. The air temperature decreases in this period, and the winter season begins in January. Mean annual precipitation can be estimated as 615 mm at Kyangjing station. Precipitation quantities generally decrease from the west to the upper parts of the valley in the northeast. The upper parts of the valley at an altitude of 5300 m a.s.l. receive almost the same amount of precipitation as Kyangjing station. This is because less moist air is conveyed to the upper part of the valley by monsoonal circulations prevailing from the south. A mountain barrier running west–east in the southern side of the valley prevents moisture from penetrating into the uppermost reaches of the valley.

The discharge regime can be classified as glacial, with maximum discharges in July and August and minimum discharges during the winter season. Winter discharge is characterized by a rather constant base flow with negligible inflows of rainwater or melts water as the air temperature is generally below the melting point.

METHODS

The TAC^D model and input data

The reservoir-based conceptual structure of TAC^D consists of separate modules (snow and glacier-, soil-, runoff generation routine) that are sequentially linked and represent the main parts of the land phase hydrological cycle (for further details see Konz *et al.*, 2006a,b, 2007).

A distributed temperature-index method is used to calculate snow- and ice melt based on potential sunshine durations and regionalized temperature values. When glaciers are present, ice melt starts as soon as the snow cover is melted and melt is enhanced compared to snow due to a reduced surface albedo. The reduced melt rate of ice beneath debris-covered parts of the glaciers is accounted for by a multiplicative factor (Braun *et al.*, 1993). Units of similar dominating runoff generation behaviour (Hydrologic Response Units, HRUs) were delineated using maps of topography and land-use, aerial photographs and a digital elevation model (DEM), as well as from repeated direct catchment surveys. Four HRUs were identified and accordingly parameterized to compute runoff generation from:

- non-glacierised areas,
- glacierised areas,
- glacierised areas with a slope of less than 3° and debris cover, and
- valley bottoms with a slope of less than 8°.

Linear reservoirs are sequentially connected to simulate runoff over these units. The characteristics of the reservoirs are defined by recession coefficients and maximum storage levels. The conceptualization of the runoff generation routine is thus kept as simple as possible while still being able to represent the most important runoff generation processes. The HRUs of type (a) and (b) consist of two storages, one representing interflow components and one for the baseflow, fast flow components are simulated if the water content exceeds the maximum storage level and the additional water is added to runoff without retention. The valley glacier tongues (c) and gravel beds of the valley bottom (d) are considered to be large storages and a single linear storage is supposed to mimic retention effects that redistribute water from the monsoon season to maintain winter discharge.

The daily model uses temperature, precipitation and potential evapotranspiration data. The model has been applied for the period 1987–2007, forced with daily precipitation and temperature data of the meteorological station in Kyangjing (Fig. 1). Since the data are subject to errors and gaps, a thorough data analysis was previously conducted, as described in Konz *et al.* (2006a), to remove inconsistencies. The model was tested over the validation period 1987–1993 (hydrological years October to September) with the best parameter sets obtained in the calibration period 1993–1997. In the first step of the calibration procedure, a manual trial-and-error calibration was performed (Konz *et al.*, 2007). The initial model parameter set was estimated according to basin characteristics, available data from literature (e.g. parameters of the snow and glacier routine) or was derived based on previous TAC^D-applications to other basins. Calibration runs were performed by adjusting only the parameters of the snow and glacier routine and the precipitation input parameters that describe corrections of the observed data and the spatial precipitations field using vertical and horizontal gradients. The initial parameters of the soil and runoff generation routines were not further adjusted as they were considered representative of the best process understanding achievable from available data and catchment knowledge. Apart from the manual trial-and-error calibration we performed around 7000 simulations in the second calibration step using parameters randomly selected parameters within the range of the values obtained from the first step, with the purpose of assessing the sensitivity of the model to parameter uncertainty. The model performance was evaluated by means of the Nash-Sutcliffe coefficient as efficiency criterion. In addition, two glacier mass balance observations available for the Yala glacier for the periods May–October 1996 (Fujita *et al*., 1998) and March 1991–March 1992 (Braun *et al*., 1993) were used in the calibration and validation phase, respectively, in order to compute the error between simulated and observed mass balance. We were thus able to identify the parameter sets that allow a satisfactory simulation of both discharge and mass balance. The suitability of MODIS snow cover maps to identify the most appropriate model parameterization was then evaluated by running simulations with two parameter sets, which reproduced discharge observations with comparable accuracy but yielded very different mass balance simulations. The first parameter set is the best for both discharge and mass balance simulations, whereas the second one provides good discharge simulation but less accurate mass balance. The snow maps of TAC^D simulated by means of these two different parameterisations were finally compared to snow cover maps of MODIS for the years 2001–2006 and assessed using the efficiency criterion described in the following section.

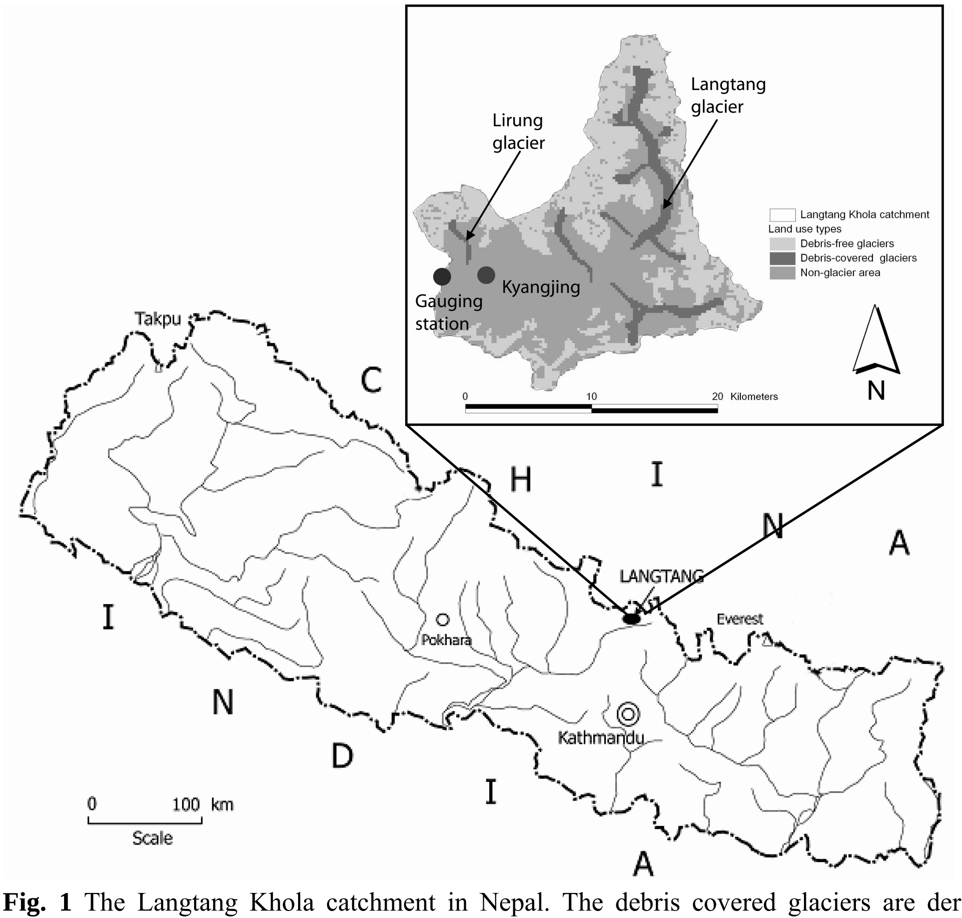

Fig. 1 The Langtang Khola catchment in Nepal. The debris covered glaciers are derived from the German Alpine Club map (Langtang Himal-Ost); the free glaciers are taken from ICIMOD's glacier inventory.
]

MODIS snow cover maps

The Moderate Resolution Imaging Spectroradiometer (MODIS) snow products range from a single swath product to an 8-day global-gridded product (see also http://modis-snow-ice.gsfc.nasa.gov for details). In this study, the daily snow cover product was used. This has a 500-m resolution and is projected on a sinusoidal grid. Snow cover products derived from MODIS are based on a band rationing of MODIS band 4 (green) (0.545–0.565 μm) and band 6 (near-infrared) (1.628–1.652 μm). These bands are used to calculate the Normalized Difference Snow Index (*NDSI*) defined as:

$$NDSI = \frac{band4 - band6}{band4 + band6} \tag{1}$$

In non-forested areas a pixel with an $NDSI \geq 0.4$ is identified as snow if the reflectance in band 2 (0.841–0.876 μm) exceeds 11% and the reflectance in band 4 is equal or higher than 10%. (Hall *et al*., 1995). In forested areas an alternative algorithm is used that includes the Normalized Difference Vegetation Index (*NDVI*) (Klein *et al*., 1998). However, when using a threshold on the *NDVI*, a forested pixel may still be classified as snow even, if the NDSI is lower than 0.4. Accordingly the accuracy of MODIS snow maps is expected to be variable, depending on the land cover characteristics. However, in the absence of a ground-based verification we assumed the MODIS snow maps to be an exact benchmark for comparison with the model simulated snow maps. The daily MODIS maps were thus used to evaluate the simulated daily snow cover extents. The model performance was defined according to an efficiency criterion that measures the goodness of fit as ratio between correctly predicted cells and total available cells having removed pixels that were cloud covered or had no measurements. This is summarized by the following equation:

$$S_{\mathrm{eff}} = \frac{n_{\mathrm{pre}}}{n_{\mathrm{cat}} - n_{\mathrm{nan}}} \cdot 100 \tag{2}$$

where: S_{eff}, snow cover efficiency [%]; n_{pre}, number of cells correctly predicted [-]; n_{cat}, number of cells in catchment [-]; n_{nan}, Number of cells in catchment with clouds or no measurements [-].

As shown in the next section, S_{eff} was calculated on a daily basis for the hydrological year 2005/2006 and in a cumulative form for the hydrological years 2001/2002 to 2005/2006.

RESULTS

The analysis of the streamflow simulations reveals a certain level of ambiguity. Figure 2 is a good example of this. It shows daily discharge simulations of the year 1995/1996 as computed by means of the two selected parameter sets. While in the recession phase both simulations show a comparable behaviour, the values simulated using ps 1 show a slightly higher intraannual variability, even if overall the simulated discharge trajectories are consistent with each other. Conversely, the two simulations show for the same year very different mass balance simulations (Fig. 3).

The unsatisfactory performance with regard to mass balance can be likely explained by looking at the differences among the parameter sets. Table 2 summarizes such differences.

The comparison of observed and simulated glacier mass balance shows that the ablation is significantly underestimated by the model run using ps 2, whereas the accumulation of snow is overestimated at high elevations (Fig. 3). Ps 2 significantly underestimated the melt water production likely due to lower values of the degree-day factor (CFMAX) and of the parameter indicating the increase of ice melt compared to snow (RMULT), as well as to a higher temperature gradient (TGRAD). Conversely, the melt beneath debris layers is simulated with a higher multiplicative factor (RMULTD), which leads to a higher melt water production of the 20% debris covered glacier areas. The underestimation of melt water production, however, was balanced out by an overestimation of the precipitation input, which compensated the volume losses of the melt simulation. The rain correction factor, PCF, and the snow correction factor, SFCF, as well as the vertical and horizontal precipitation gradients (PGRAD and PHORIZGRAD), are indeed higher than in ps 1.

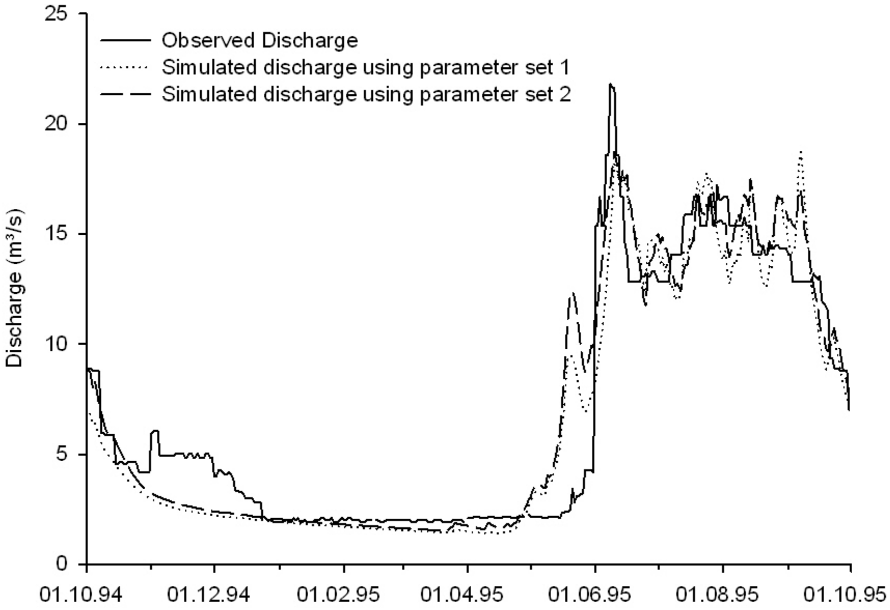

Fig. 2 Comparison of measured (solid) and simulated (dotted and dashed) discharge for the hydrological year 1994/1995).

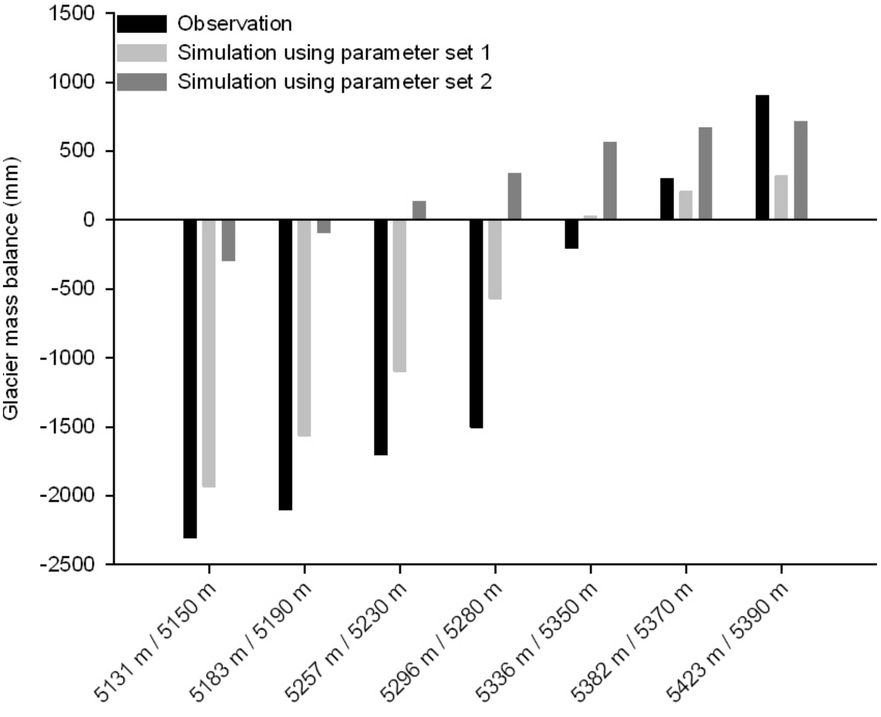

Fig. 3 Comparison of measured and simulated glacier mass balances of Yala glacier (May–October 1996). The two simulated glacier mass balances were computed with parameter sets used for the simulation of streamflow shown in Fig. 2. The first altitude on the x-axis is the altitude of the grid cell of the DEM that covers the measurement point (second altitude value).

Table 2 Differences between the two parameter sets. Only parameters relevant to snow- and ice melt and to temperature and precipitation redistribution are listed.

	Ps 1	Ps 2
PCF	1.05	1.3
PGRAD	0.04	0.045
PHORIZGRAD	–0.03	–0.02
TGRAD	–0.5	–0.55
SFCF	1.2	1.4
CFMAX	7.0	4.0
RMULT	1.4	1.2
RMULTD	0.3	0.5

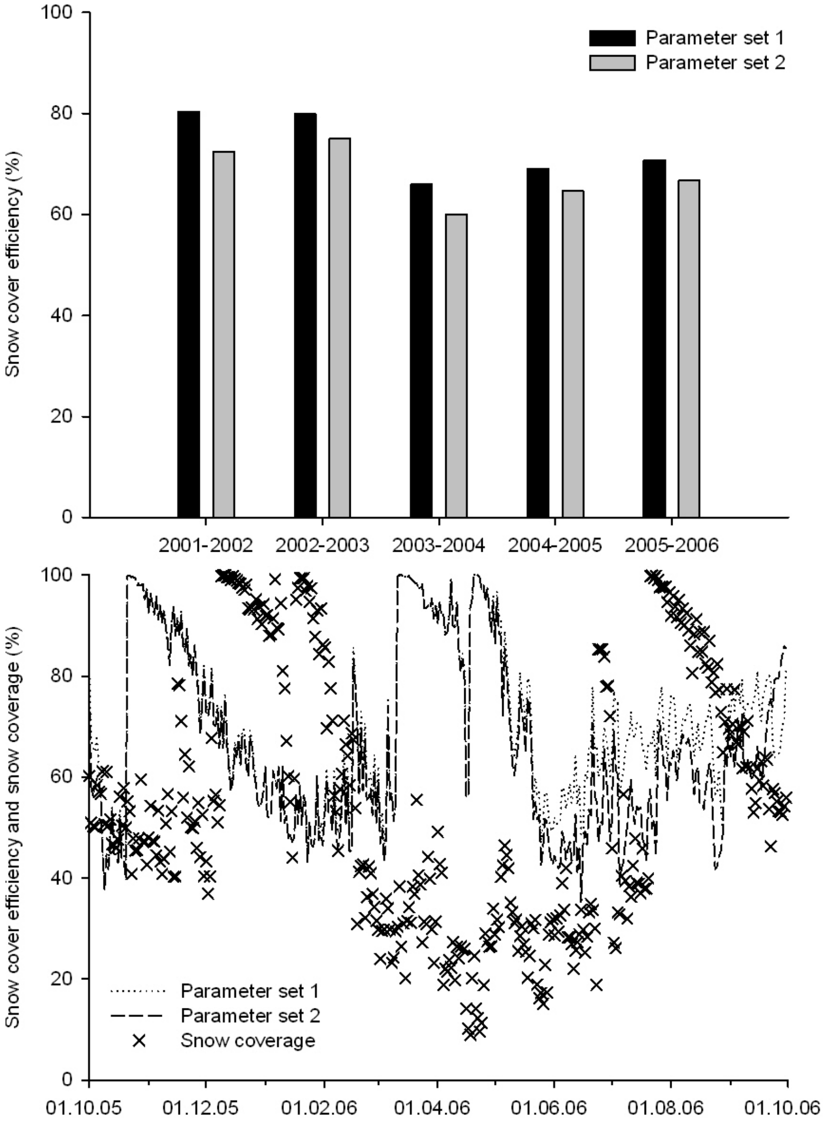

Fig. 4 Snow cover efficiencies of the two parameter sets as computed by equation (2).

Figure 4 compares the snow cover efficiencies of the two parameter sets as derived from the comparison with the MODIS data and measured according to equation (2). Ps 1 delivered for all five analysed years better overall snow coverage simulations than ps 2, which seems to be affected by a constant negative bias with respect to ps 1 (Fig. 4, upper panel). With respect to the intraannual variability (Fig. 4, lower panel) ps 1 was more efficient than ps 2, mainly during the summer, whereas it showed only a slightly better performance during the pre-monsoon season. The lower panel in Fig. 4 also shows the snow coverage of the entire catchment, which is in general relatively low and mainly limited to higher elevations, also showing frequent fluctuations and very few days with total snow coverage. Particularly in the period where snow cover is large, the model seems to provide lower efficiencies, thus suggesting some limitations of the accumulation model component, which is based essentially on elevation-based gradients of precipitation and temperature.

DISCUSSION AND CONCLUSION

The applicability of MODIS snow cover data to identify parameter sets for modelling glaciated catchments was demonstrated for remotely located highly glacierised basins. This was achieved using data of the Langtang Khola catchment (Himalaya) for which discharge and mass balance observations available for different seasons allowed a calibration focusing on multiple variables. We identified two parameter sets by means of Monte Carlo simulations that delivered comparable discharge values, but very different mass balance simulations. Ps 1 provided good discharge and mass balance simulations, whereas ps 2 significantly underestimated ablation, but compensated for it by an overestimation of liquid precipitation. While the model using ps 2 was not able to correctly capture the melt dynamics, as observed by remotely sensed snow maps, it could still simulate the observed discharge as efficiently as the model that used ps 1. This result points at the problem of multiplicity of parameter sets – also known in the literature as “equifinality” – which can be tackled and eventually solved by calibrating the model against multiple variables, which allow for assessing the internal consistency. The glacier mass balance provided us with a useful additional evaluation criterion at the investigated area, which enabled the assessment of a parameterisation that balanced the melt dynamics components of the model with those related to the spatial precipitation inputs and to the accumulation. Therefore, a more consistent parameter set selection than that obtained for calibration discharge data only can be achieved. This study proved that snow cover maps derived from satellite images can play the same role, while being much more frequently available than glacier mass balance data, which are rarely available in the most remote mountainous regions of the world, such as the Himalayan catchments. The use of daily MODIS snow cover maps allowed the identification of ps 1 as more efficient than ps 2 in simulating the snow cover at the annual scale. However, both parameter sets delivered relatively low snow cover efficiencies within the year and compared to simulations currently performed in the European Alps (Finger, personal communication). This could be partly explained by the more complex snow patterns in the Himalayas. In the headwaters of the European Alps, the snow cover persists, at least for basins at high elevations, throughout the entire winter with only little changes in its extent, whereas in the Himalayas the snow coverage changes frequently due to the concurrent time of accumulation and ablation. Snow cover could thus be present in the morning, but already melted away in the evening. Furthermore, precipitation falls mainly during the monsoon season, which is characterized by high temperatures, making the snow coverage very sensitive to temperature gradients. A correct representation of the latter and, more in general, of the spatial temperature fields, is hard to achieve in areas with uneasy access with only one climate station at the valley bottom. Thus, efficiency values as in the European Alps should not be expected. However, even if the overall efficiency is relatively low and quit fluctuating, the use of MODIS snow maps provides an additional reference data set to constrain the selection of model parameters to combinations that provide a higher degree of internal consistency of the model.

Acknowledgments We highly acknowledge the collaboration with the Snow and Glacier Hydrology Unit of the Department of Hydrology and Meteorology in Nepal. They are collecting, maintaining and processing the meteorological and discharge data. Dr Arun Shrestha supported this study with valuable discussions and background information on the catchment.

REFERENCES

Braun, L. N., Grabs, W. & Rana, B. (1993) Application of a conceptual precipitation runoff model in the Langtang Khola basin, Nepal Himalaya. In: *New Approaches to Hydrological Prediction in Data Sparse Regions* (Proc. Symp. Town, Countrie, 3–6 September 1993), 221–237. IAHS Publ. 218. IAHS Press, Wallingford, UK.

Hall, D. K., Riggs, G. A. & Salomonson, V. V. (1995) Development of methods for mapping global snow cover using Moderate Resolution Imaging Spectroradiometer (MODIS) data. *Remote Sens. Environ.* **54**, 127–140.

Hall, D. K., Riggs, G. A., Salomonson, V. V., DiGirolamo, N. E. & Bayr, K. J. (2002) MODIS snow-cover products. *Remote Sens. Environ.* **83**, 181–194.

Immerzeel, W. W., Droogers, P., de Jong, S. M. & Bierkens, M. F. P. (2009) Large-scale monitoring of snow cover and runoff simulation in Himalayan river basins using remote sensing. *Remote Sens. Environ.* **113**, 40–49.

Kattelmann, R. (1993) Role of snowmelt in generating streamflow during spring in east Nepal. In: *New Approaches to Hydrological Prediction in Data Sparse Regions* (Proc. Symp., 3–6 September 1993), 103–111. IAHS Publ. 218. IAHS Press, Wallingford, UK.

Klein, A. G., Hall, D. K. & Riggs, G. A. (1998) Improving snow-cover mapping in forests through the use of a canopy reflectance model. *Hydrol. Processes* **12**, 1723–1744.

Konz, M., Braun, L., Uhlenbrook, S., Grabs, W. & Shrestha, A. (2006a) Runoff from Nepalese Head Watersheds based on Measurements and Modelling. *IHP/HWRP-Bericht, Heft 4*, ISSN, 1614–1180.

Konz, M., Braun, L., Uhlenbrook, S., Shrestha, A. & Demuth, S. (2006b) Regionalisation of a distributed catchment model for highly glacierized Nepalese headwatersheds, In: *Water Resource Variability: Processes, Analyses and Impacts* (Proc. 5th FRIEND World Conf., 27 November–1 December 2006, Havana, Cuba). IAHS Publ. 308. IAHS Press, Wallingford, UK.

Konz, M., Braun, L., Uhlenbrook, S., Shrestha, A. & Demuth, S. (2007) Implementation of a process-based catchment model in a poorly gauged, highly glacierized Himalayan headwater, *Hydrol. Earth Syst. Sci.* **11**, 1323–1339.

Konz, M. & Seibert, J. (2010) On the value of glacier mass balances for hydrological model calibration. *J. Hydrol.* doi:10.1016/j.jhydrol.2010.02.025.

Moribayashi, S. (1974) On the characteristics of Nepal Himalayan glaciers and their recent variation. *Seppyo* **36**, 11–21 (in Japanese with English abstract).

Parajka, J. & Blöschl, G., (2006) Validation of MODIS snow cover images over Austria. *Hydrol. Earth System Sci.* **10**, 679–689.

Parajka, J. & Blöschl, G. (2008) The value of MODIS snow cover data in validating and calibrating conceptual hydrologic models. *J. Hydrol.* **358**, 240–258.

Rango, A. (1992) Worldwide testing of the snowmelt runoff model with application for predicting the effects of climate change. *Nordic Hydrol.* **23**, 155–172.

Shiraiwa, T., Ueno, K. & Yamada, T. (1992) Distribution of mass input on glaciers in the Langtang Valley, Nepal Himalayas. *Bull. Glacier Res.* **10**, 21–30.

Sakai, A., Fujita, K. & Kubota, J (2004) Evaporation and percolation effect on melting at debris-covered Lirung Glacier, Nepal Himalayas. *Bull. Glacier Res.* **21**, 9–15.

Seko, K. (1987) Seasonal variation of altitudinal dependence of precipitation in Langtang Valley, Nepal Himalayas. *Bull. Glacier Res.* **5**, 41–47.

Simic, A., Fernandes, R., Brown, R., Romanov, P. & Park, W. (2004) Validation of VEGETATION, MODIS, and GOES+SSM/I snow cover products over Canada based on surface snow depth observations. *Hydrol. Processes* **18**, 1089–1104.

Ueno, K. & Yamada, T. (1990) Diurnal variation of precipitation in Langtang Valley, Nepal Himalayas. *Bull. Glacier Res.* **8**, 93–101.

Viviroli, D., Dürr, H. H., Messerli, B., Meybeck, M. & Weingartner, R. (2007) Mountains of the world, water towers for humanity: Typology, mapping, and global significance. *Water Resour. Res.* **43**, W07447, doi:10.1029/2006WR005653.